ISSN 2229-5518

The Formation of the High T_c Phase of Melt Quenched $Bi_{1.6}Pb_{0.4}Sr_2Ca_2Cu_3O_y$

Shirley T. Palisoc, Michelle T. Natividad, Phebe P. Mendoza

Abstract— The melt quench method was applied in the fabrication of $Bi_{1.6}Pb_{0.4}Sr_2Ca_2Cu_3O_y$ superconducting ceramics. The effects of melting the lead doped BSCCO were investigated using the scanning electron microscope and energy dispersive spectroscope (SEM/EDAX), differential thermal analyzer (DTA), x-ray diffractrometer (XRD) and magnetic susceptibility (χ-T) analyses. The results showed that the superconducting phase appeared even in the precursor samples. Glass forming tendency is also remarkably retarded. Sintering at 840°C for 24 hours completely vanished this glass forming ability. The critical temperature (T_c) onset was strongly dependent on the amount of non-superconducting impurities, grain size and intensity of the endothermic peak that affects the phase formation in the partially melted state.

Index Terms— melt quench, precursor, sintering, critical temperature, superconductor, ceramic

1 Introduction

Superconductivity remained a much studied phenomenon for more than half a century after its discovery. A great deal of experimental information was gathered on its occurrence and its properties and several useful theories were developed. Different methods were also applied for fabricating superconducting materials. Among these were the alkoxide route, citrate gel process, coprecipitation technique, combustion method, freeze dying, floating zone method, solgel, solid state reaction method, melt quench method and spray pyrolysis method (Yoo et al 2004). Efforts were also made to enhance and increase the volume fraction of the high T_c phase by several processes like low tremperature annealing, long time sintering, sintering under low oxygen partial pressure and lead (Pb) addition. The lead addition was found to be the most efficient (Asamo et al 1989, Yoshizaki et al 1990).

This paper presents a simple way of fabricating Pb doped BSCCO superconductiong glass ceramics known as the melt quench method. The method involves metling the raw materials in a crucible and then quenched to room temperature. The study deals with the characterization of the melt quenched samples and the determination of the relationship between the melt quenched precursors and the sintered samples.

2 Methods

The nominal composition of $Bi_{1.6}Pb_{0.4}Sr_2Ca_2Cu_3O_y$ was prepared from Bi_2O_3, PbO, $SrCO_3$, $CaCO_3$ and CuO. The mixed powder was melted in an alundum crucible in an electric furnace at a temperature of 1080°C (Harada et al 1992) for 5 minutes. The melts were poured immediately onto a stainless steel plate and then cooled to room temperature. The obtained samples were characterized using the SEM/EDAX, DTA and XRD. SEM/EDAX JEOL JSM35C was used to analyze the crystal grain structure and the micro composition of the precursors. X-ray diffraction measurement was carried out using the RIGAKU X-ray diffractometer. The diffractometer used CuKα radiation with a wavelength of 1.541838Å, generator tension of 30kV and generator current of 15mA. The scanning angle ranged from 2° to 41°. For the differential thermal analysis, the Perkin and Elmer Thermal Analyser was used. The reference material used for temperature difference was aluminum oxide (Al_2O_3).

The melt quenched precursors were weighed and divided to approximately 4 grams each. Each 4 gram powder was pelletized to 6 tons for 3 minutes using the hydraulic press. Each pellet was approximately 2 cm in diameter and 2.5 mm in thickness. All pellets were sintered at a constant temperature of 840°C for 24 hours. The samples were left to cool inside the furnace to room temperature. The samples were characterized by SEM/EDAX, DTA, XRD and χ-T tests.

3 Results

The XRD patterns for the melt quenched precursor (**Fig. 1a**) show that there is a coexistence of high T_c peaks corresponding to the 2223 and 2212 phases, respectively. A prominent peak at $2\theta = 30°$ is observed in all the precursor samples. According to Komatsu et al (Komatse et al 1988), this peak is ascribable to the glassy phase which indicates that this phase is largely included in the melt quenched samples. Peaks attributed to the impurity Ca_2CuCO_3 and CaO are observed around $2\theta = 36.4°$ and $2\theta = 37.5°$, respectively. These peaks are present in all trials and no significant change in its intensity is observed. The peak at $2\theta = 36.4°$ disappeared after sintering in trial 3. The peak around $2\theta = 37.5°$ disappeared after sintering for trials 2 and 3 and a very minimal amount is left for trial 1. This can be attributed to the melting of the secondary phases Ca_2CuCO_3 and CaO at around 700°C – 750°C as shown in the DTA results. Peaks resulting from a semiconducting phase (2201) occurring at $2\theta = 21.9°$ and $2\theta = 7.1°$ are found in all precursors. This peak also disappeared after sintering. This may be attributed to the formation of the 2212 phase from

- *Shirley Tiong Palisoc, Ph.D. In Materials Science is a professor at the Department of Physics, De La Salle University – Manila, Philippines. E-mail: shirley.palisoc@dlsu.edu.ph*
- *Michelle Natividad, Ph.D. in Physics is an assistant professor at the Department of Physics, De La Salle University – Manila, Philippines. E-mail: natividad@dlsu.edu.ph*
- *Phebe Mendoza, M.S. in Physics is a faculty member of Holy Angel University, Pampanga, Philippines*

2201 phase during annealing at around 800°C (Kanai et all 1988).

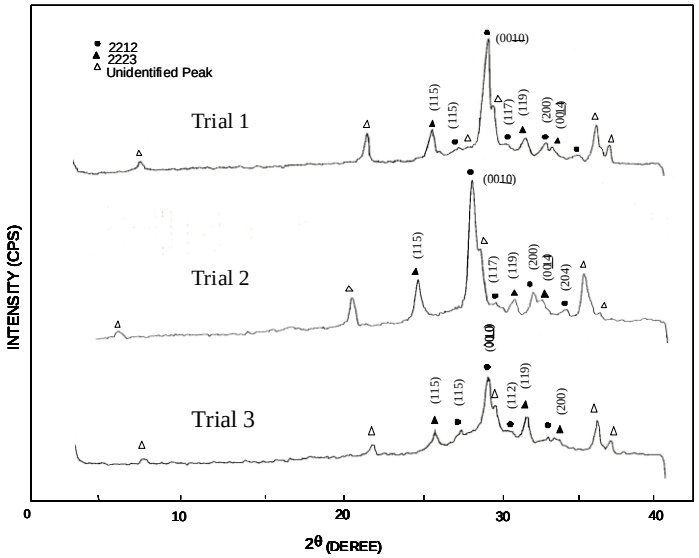

Fig. 1a XRD patterns of precursor samples

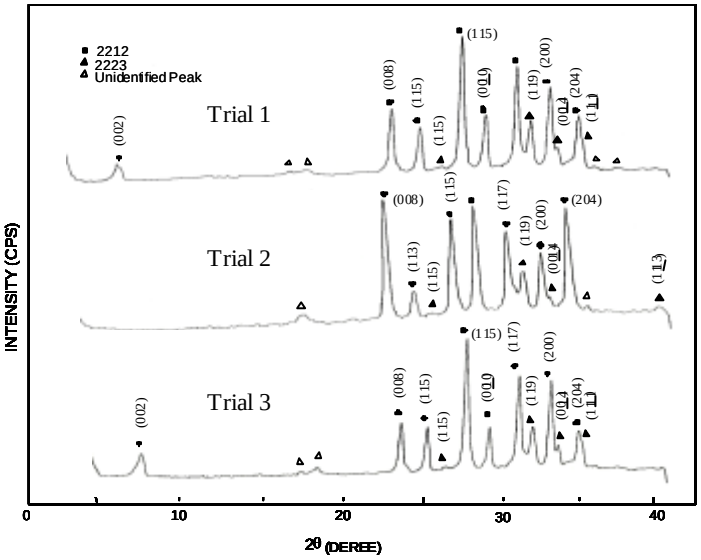

Fig. 1b XRD patterns of sintered samples

Peaks at (115), (119) and (0014) corresponding to the 2223 phase is again observed after sintering and most of the remaining peaks are attributed to the more stable phase which is the 2212 phase (**Fig. 1b**). The presence of the impurity peak at $2\theta = 17.6°$ (Ca_2PbO_4) arising from the addition of lead in the system and at $2\theta = 36.4°$ (Ca_2CuCO_3) are very minimal. Data show a predominance of 2212 phase over 2223 phase for the sintered samples.

Most thermal events in the DTA scans of the precursor samples can be matched, suggesting that the crystallization processes for the three trials are essentially the same (**Fig. 2a**). Glass transition (T_g) at around 250°C – 398°C is observed before three exothermic peaks. Two smaller endothermic peaks precede the main melting event at around 770°C- 860°C. The pattern of this DTA curve is very similar to that of the melt quenched sample reported by Sato et al (Sato et al 1989), although the endothermic and exothermic temperature peaks are different. The first exothermic peak after the glass transition can be attributed to the crystallization of the 2201 phase. It is noted that the second exothermic peak is always found to be strongest (Holesinger et al 1992). The reason for this is not yet clear. The second exothermic peak can be attributed to the formation of the secondary phase such as CaO, Ca_2CuO_3 and some undissolved Bi_2O_3. The third exothermic peak can be attributed to the crystallization of the 2212 phase. The endothermic peaks after the exotherms can be attributed to the melting of the secondary phases and partial melting of the 2201 phase. The exothermic peak around 790°C corresponds to the formation of 2212 phase and the subsequent formation of the 2223 phase enhanced by the partial melting of the 2201 phase (Sato et al 1989). This exothermic peak is followed by endotherms indicating the melting of the different phases.

It is noted that the endothermic peaks after the three exotherms are nearly identical. However, some minor differences in their scans suggest that a small amount of zinc and aluminum, as shown in EDAX results, inhibit the formation in the partially melted state (Holesinger et al 1992). An exothermic peak still appeared after the endothermic event for trial 1. This is likely attributed to an unknown phase formation or formation of 2223 phase since partial melting occurred around 830°C – 879°C (Hatano et al 1988).

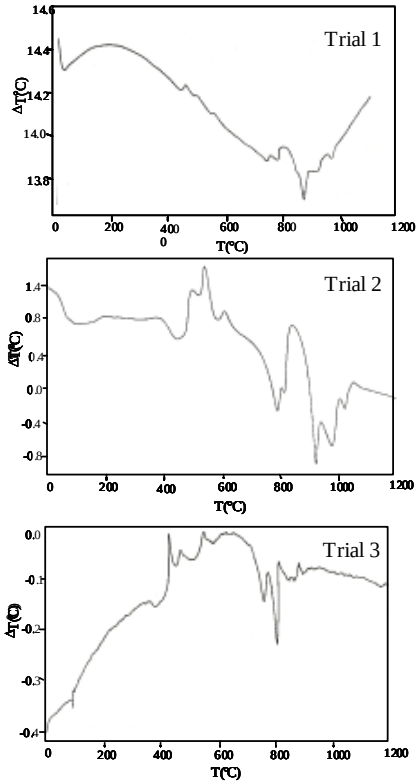

Fig. 2a DTA patterns of precursor samples

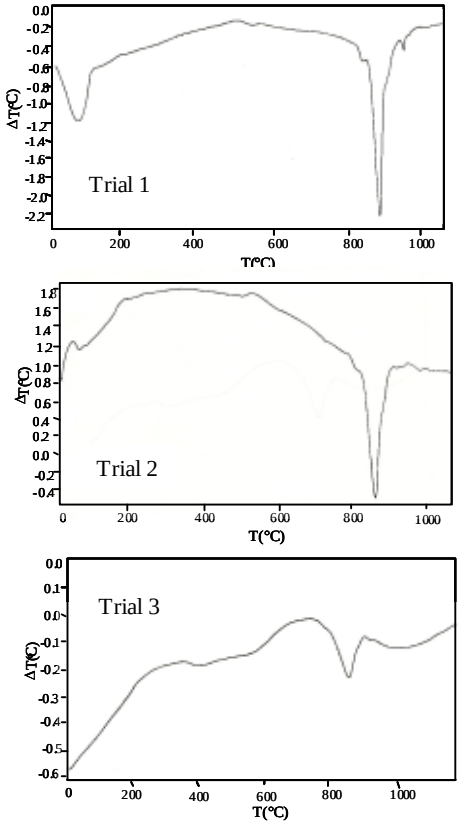

Fig. 2b DTA patterns of sintered samples

The DTA curves for the sintered samples are shown in Fig. **2b**. The three curves show an endothermic peak at temperature between 820°C – 892°C. These endothermic peaks are attributed to the melting point of the samples. The peak at 90°C – 150°C may be due to the thermal instability of the system which occurs during the start of the run and not a phase transition of the sample. XRD results for the sintered samples show quite a stable 2212 phase as verified by DTA since no exothermic peak appears in the scan. At temperature 951.79°C for trial 1 an endothermic peak is observed. The reason for this is still unknown. This probably can be attributed to the melting of the Cu_2CaCO_3 and CaO phases.

Fig. 3a shows the EDAX results for the precursor samples. The sample in trial 1 contained larger amounts of Ca and Sr compared to the rest of the trials. In trial 3, on the other hand, the sample showed large amounts of Zn, Al and Fe. These came from the CuO powder used as starting material.

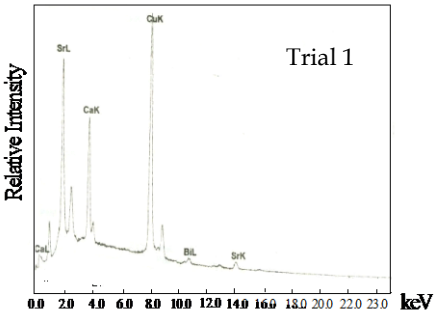

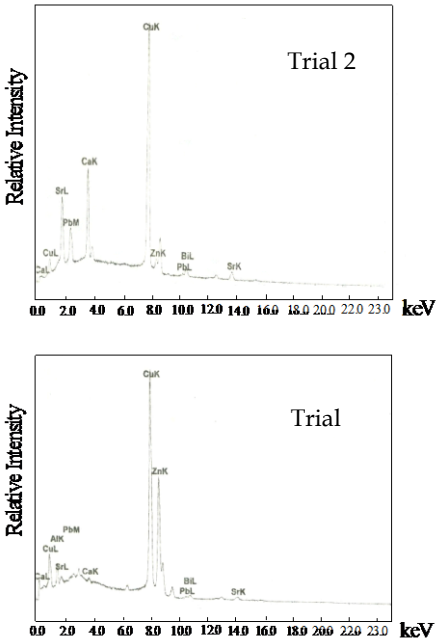

Fig. 3a EDAX patterns of the precursor samples

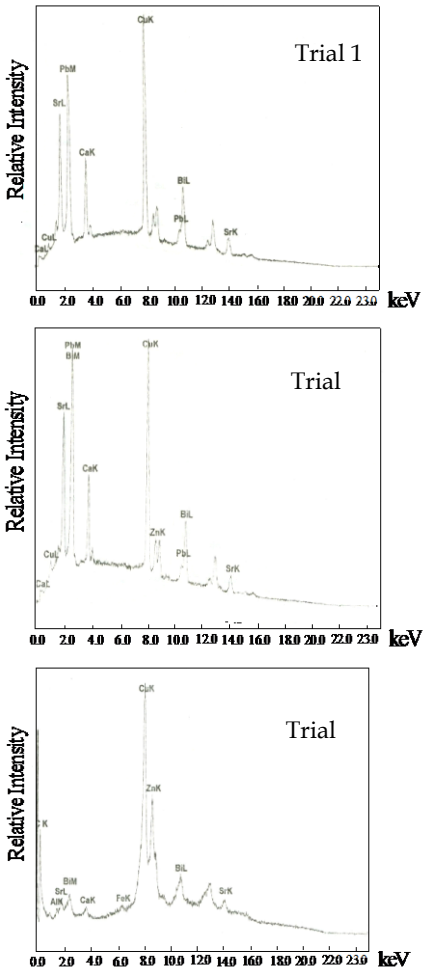

Fig. 3b EDAX patterns of sintered samples

Fig. **3b** shows the EDAX results for the sintered samples. It can be seen that in trial 3, the impurity did not disappear even after sintering. The relative amount of Bi, Sr, Ca, Cu and Pb of the three trials decreased after sintering. This could be explained by the removal of the glass phase after sintering as verified by the XRD results.

Fig. 4 shows the magnetic susceptibility curves of the sintered samples. The ac susceptibility for trial 1 shows a two step transition: a small one of the high T_c phase (106K) and a large step, one of the low T_c phase (68K). DTA results show a broad exotherm at approximately 930°C for trial 1. This peak is attributed to the formation of the high T_c phase. DTA results for trials 2 and 3 show the absence of this peak. Formation of high T_c phase in trial 1 is distinct and is related to this small step size which is not seen in the χ-T curve of trial 2. XRD results also show that trial 1 has higher peak intensity and small amount of Ca_2PbO_4. The high T_c phase in trial 2 as identified by XRD results is verified by ac- susceptibility measurement showing a signal of high T_c phase at around 80K. The decrease in the T_c onset can be attributed to the large amount of Ca_2PbO_4 and non superconducting phases. Trial 3 has the lowest T_c onset (66K). XRD result shows that it has the highest percentage of coexisting low and high T_c peaks.

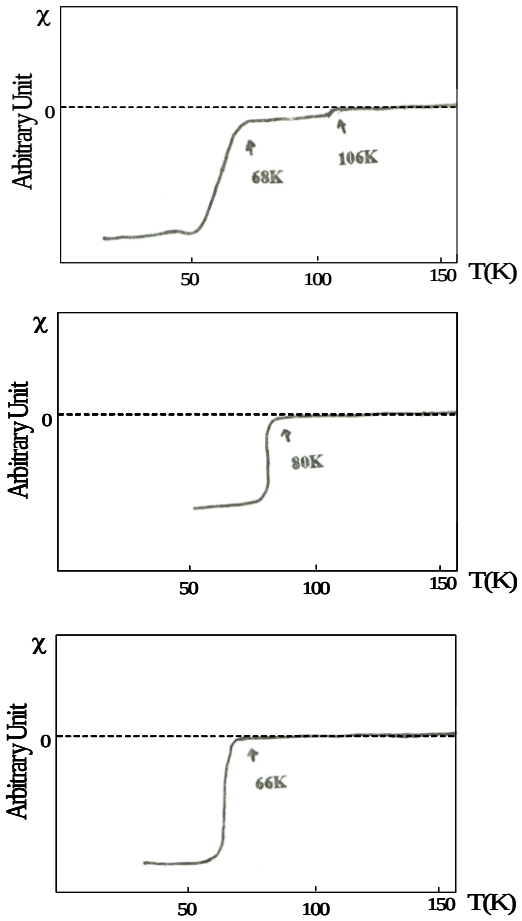

Fig. 4 Complex Susceptibility patterns of the sintered samples

Fig. 5a shows the SEM micrographs of the precursor samples. The needle like structure is abundant for all trials. These needle shape grain may be an intermediate state of non-superconducting phase (Shah et al 1988). This is consistent with the XRD results of the precursor samples. **Fig. 5b** shows the SEM micrographs of the sintered samples. As observed from the photographs, the sample in trial 1 (T_c onset of 106K) has advanced crystal growth as compared to trial 2 with bigger grain size and lower T_c onset of 80K. The sample in trial 3 (T_c onset of 66K) has the least crystallization development. The change in microstructure is attributed to the change in thermal reaction. High T_c phase is formed during an endothermic reaction. A weak endothermic reaction shows a slow nucleation thus the high T_c phase slowly develops (Nasu et al 1990). DTA for sintered samples for trial 1-3 show a decrease in the endothermic sharpness and intensity thus nucleation slowly develops. This is consistent with the SEM results. Small grain size is said to preferably attain High T_c end (Nasu et al 1990). This is also consistent with the χ-T results. As the endothermic peak decreases from trial 1-3, grain size increase and T_c onset decreases.

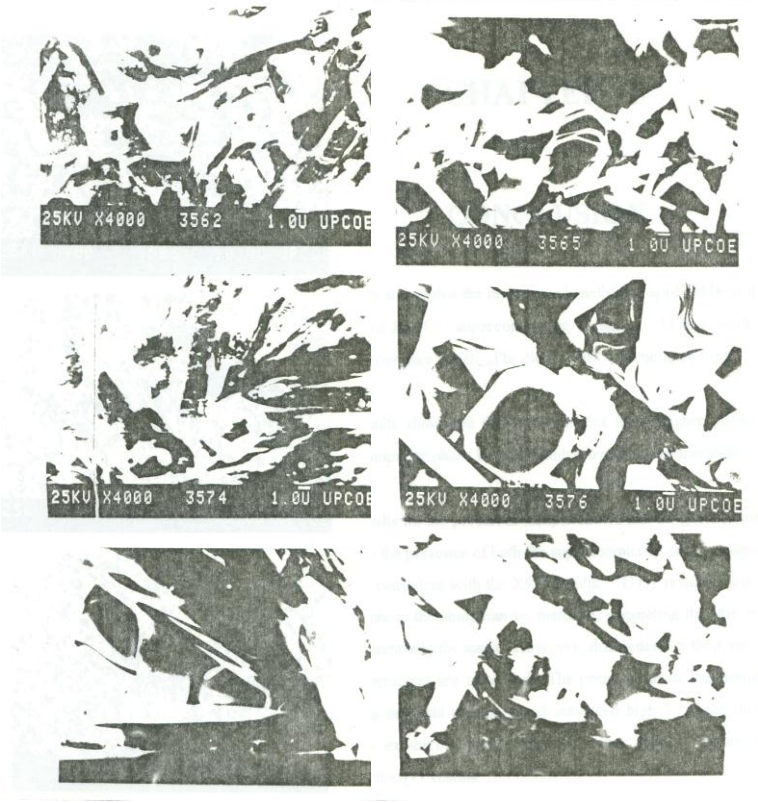

(a) **(b)**

Fig. 5 SEM micrograpahs of the **(a)** precursor samples and **(b)** sintered samples of trials 1-3.

4 DISSCUSSION

In this paper, the highest onset critical temperature for $Bi_{1.6}Pb_{0.4}Sr_2Ca_2Cu_3O_y$ ceramic is 106K. XRD results show that the precursor that has a higher intensity peak and less percentage impurity phase lead to a higher transition temperature. SEM results for the precursor sample shows that the glass forming ability is decreased due to the presence of both the superconducting and non-superconducting phases. This is consistent with the XRD results. DTA results show that most of the thermal events in the study can be matched, suggesting that the crystallization processes are essentially the same. However, differences in their endothermic and exothermic temperatures are observed. The presence of an exothermic peak after the main melting suggests a greater and enhanced high T_c phase formation. The absence of this exothermic peak suggests a less high T_c phase formation as collaborated by the χ-T results. The endothermic peak increased as T_c onset increased suggesting a faster nucleation and a decrease in grain size. This is consistent with the SEM results. This agrees with the results of Nasu et al (Nasu et al 1990) where smaller grain size is preferable in having high critical temperature. EDAX results also show several impurities. These impurities inhibit the formation of the 2212 and 2223 phases and affect the phase formation in the partially melted state.

The precursor that has the sharpest endothermic peak, smallest grain size, least amount of impurities and the highest peak intensity lead to a higher transition temperature.

REFERENCES

[1] Asano T, Tanaka Y, Fukutomi M, Jikihara K & Maeda H. 1989. Properties of Pb-Doped Bi-Sr-Ca-Cu-O Superconductors Prepared by the Intermediate Pressing Process. *Japanese Journal of Applied Physics*. 28:L595-L597.

[2] Harada R, Yoshinari O & Tanaka K. 1992. Crystallization of Superconducting Phases in Melt-Quenched and Annealed $Bi_{1.6}Pb_{0.4}Sr_2Ca_{n-1}Cu_nO_y$ (n=1 to 4) Ceramics. *Japanese Journal of Applied Physics*. 31:2420-2426.

[3] Hatano T, Aota K, Ikeda S, Nakamura K & Ogawa K. 1988. Growth of the 2223 Phase in Leaded Bi-Sr-Ca-Cu-O System. *Japanese Journal of Applied Physics*. 27:L2055-L2058.

[4] Holesinger TG, Miller DJ & Chumbley LS. 1992. Crystallization of Bi-Sr-Ca-Cu-O glasses in oxygen. *Journal of Materials Research*. 7:1658–1671.

[5] Holesinger TG, Miller DJ, Fleshler S & Chumbley LS. 1992. Processing of Bi-Sr-Ca-Cu-O Glasses Using Platinum and Alumina Crucibles. *Journal of Materials Research*. 7:2035-2039.

[6] Kanai T, Kumagai T, Soeta A, Suzuki T, Aihara K, Kamo T & Matsuda S. 1988. Crystalline Structures and Superconducting Properties of Rapidly Quenched $BiSrCaCu_2O_x$ Ceramics. *Japanese Journal of Applied Physics*. 27:L1435-L1438.

[7] Komatsu T, Sato R, Hirose C, Matusita K & Yamashita T. 1988. Preparation of High-T_c Superconducting Bi-Pb-Sr-Ca-Cu-O Ceramics by the Melt Quenching Method. *Japanese Journal of Applied Physics*. 27:L2293-L2295.

[8] Nasu H, Kuriyama N & Kamiya K. 1990. Influences of Nb Addition on Superconducting Properties in Bi, Pb-Sr-Ca-Cu-O Glass-Ceramics. *Japanese Journal of Applied Physics*. 29:L1415-L1418

[9] Sato R, Komatsu T, Matushita K & Yamashita T. 1989. Superconducting Properties of Bi-Pb-Sr-Ca-Cu-O Ceramics Prepared by the Melt-Quenching Method. *Japanese Journal of Applied Physics*. 28:L583-L586.

[10] Shah SI & Jones GA. 1988. Growth and microstructure of Bi-Sr-Ca-Cu-O thin films. *Applied Physics Letters*. 53:429-431.

[11] Yoshizaki R, Ikeda H, Yoshikawa K & Tomita N. 1990. Properties of Pb-Doped Bi-Sr-Ca-Cu-O Superconductors Prepared by a Hot-Press Method. *Japanese Journal of Applied Physics*. 29:L753-L756.